Proc. Natl. Acad. Sci. USA
Vol. 96, pp. 4198–4203, March 1999
Plant Biology

Genetic evidence for the role of GDP-mannose in plant ascorbic acid (vitamin C) biosynthesis

PATRICIA L. CONKLIN*†, SUSAN R. NORRIS*‡, GLEN L. WHEELER§, ELIZABETH H. WILLIAMS*¶, NICHOLAS SMIRNOFF§, AND ROBERT L. LAST*‡

*Boyce Thompson Institute for Plant Research and Section of Genetics and Development, Cornell University, Ithaca, NY 14853-1801; and §Hatherly Laboratories, School of Biological Sciences, University of Exeter, Prince of Wales Road, Exeter EX4 4PS, United Kingdom

Communicated by André T. Jagendorf, Cornell University, Ithaca, NY, January 25, 1999 (received for review November 30, 1998)

ABSTRACT **Vitamin C (L-ascorbic acid; AsA) acts as a potent antioxidant and cellular reductant in plants and animals. AsA has long been known to have many critical physiological roles in plants, yet its biosynthesis is only currently being defined. A pathway for AsA biosynthesis that features GDP-mannose and L-galactose has recently been proposed for plants. We have isolated a collection of AsA-deficient mutants of *Arabidopsis thaliana* that are valuable tools for testing of an AsA biosynthetic pathway. The best-characterized of these mutants (*vtc1*) contains ≈25% of wild-type AsA and is defective in AsA biosynthesis. By using a combination of biochemical, molecular, and genetic techniques, we have demonstrated that the *VTC1* locus encodes a GDP-mannose pyrophosphorylase (mannose-1-P guanyltransferase). This enzyme provides GDP-mannose, which is used for cell wall carbohydrate biosynthesis and protein glycosylation as well as for AsA biosynthesis. In addition to genetically defining the first locus involved in AsA biosynthesis, this work highlights the power of using traditional mutagenesis techniques coupled with the *Arabidopsis* Genome Initiative to rapidly clone physiologically important genes.**

Vitamin C (L-ascorbic acid; AsA), one of the best known of the plant metabolites, is present in millimolar concentrations in most plant tissues and has many proposed roles in plant growth and metabolism. AsA has the capacity to directly eliminate several different reactive oxygen species, maintain α-tocopherol in the reduced state, and act as a substrate for AsA peroxidase. It also preserves the activity of a number of different enzymes by maintaining prosthetic group metal ions in the reduced state (1). Given the importance of AsA in these and other roles and its abundance in all plants tested, it is surprising that its biosynthetic pathway in plants has remained enigmatic. However, significant progress has recently been made toward understanding AsA biosynthesis in plants (2).

Before this recent work, two different plant AsA biosynthetic pathways had been proposed (3). One is based on the pathway documented in animals such as rat, which proceeds with inversion of the carbon skeleton of the precursor glucose. An analogous pathway has been proposed for plants, with D-galacturonate and L-galactono-1,4-lactone as two key intermediates (1). However, there are radioactive tracer data indicating that inversion of the glucose carbon skeleton does not occur during AsA biosynthesis in higher plants (4). A noninversion pathway was proposed that invokes D-glucosone and L-sorbosone as intermediates (5, 6), but no recent evidence has been reported for this pathway (2).

Wheeler *et al.* (2) recently proposed a plant AsA biosynthetic pathway that does not predict inversion of the carbon skeleton of glucose, with D-mannose and L-galactose as key intermediates (Fig. 1). Supporting the hypothesis that mannose is involved in the pathway, when *Arabidopsis* leaves are fed with [^{14}C]mannose, ≈10% of the label appears in AsA within 4 hr (2). Furthermore, it was shown that L-galactose can be synthesized by a previously described GDP-D-mannose-3,5-epimerase activity (Fig. 1, step 5; refs. 7 and 8), which was detected in both pea and *Arabidopsis* (2). By using both *Arabidopsis* and pea extracts, Wheeler *et al.* (2) demonstrated that L-galactono-1,4-lactone can be produced from L-galactose by a newly identified L-galactose dehydrogenase activity (Fig. 1, step 7), and this reaction proceeds without carbon skeleton inversion. L-galactono-1,4-lactone can then be converted to AsA by the well-documented L-galactono-1,4-lactone dehydrogenase enzyme (9–11). A fascinating implication of this pathway is that it plays several key roles in plant metabolism: in addition to serving as intermediates for AsA biosynthesis, a number of the intermediates in this proposed pathway are utilized in cell wall biosynthesis and protein glycosylation.

Although biochemical evidence has been gathered for the pathway in Fig. 1, *in vivo* support for this scheme has been lacking. We have taken a complementary genetic approach to unraveling AsA biosynthesis in higher plants by isolation and analysis of a collection of AsA-deficient *vtc* (for vitamin C) *Arabidopsis* mutants (ref. 12; P.L.C., S. A. Saracco, S.R.N., and R.L.L., unpublished data). These mutants should further our understanding of the roles of AsA in plants and allow critical testing of the newly proposed AsA biosynthetic pathway. The best characterized of these mutants, *vtc1-1*, was isolated by its sensitivity to the air pollutant ozone and was found to be defective in the conversion of glucose to AsA (12, 13). In support of the newly proposed AsA biosynthetic pathway, in this report we present evidence that the *VTC1* locus encodes GDP-mannose pyrophosphorylase (EC 2.7.7.13; mannose-1-phosphate guanyltransferase; Fig. 1, step 4). This enzyme, which was predicted by the proposed pathway, produces GDP-mannose used for cell wall carbohydrate biosynthesis, protein glycosylation, and AsA biosynthesis.

MATERIALS AND METHODS

Plant Culture. The *Arabidopsis thaliana* used for mapping and transformation, and the T_1 transgenics were grown in "Cornell Mix" soil (14). F_3 families used for mapping and the T_1 transgenics were grown in a light room (80–100 μmol·m^{-2}·sec^{-1} light provided by 400-W metal halide bulbs, 20–22°C,

The publication costs of this article were defrayed in part by page charge payment. This article must therefore be hereby marked "*advertisement*" in accordance with 18 U.S.C. §1734 solely to indicate this fact.

PNAS is available online at www.pnas.org.

Abbreviations: AsA, L-ascorbic acid; BAC, bacterial artificial chromosome; wt, wild type; EST, expressed sequence tag; EMS, ethyl methanesulfonate.

†To whom reprint requests should be addressed at: Boyce Thompson Institute for Plant Research, Tower Road, Ithaca, NY 14853-1801. e-mail: PLC3@cornell.edu.
‡Present address: Cereon Genomics, LLC, 270 Albany Street, Cambridge, MA 02139.
¶Present address: Section of Genetics and Development, Cornell University, Ithaca, NY 14853-1801.

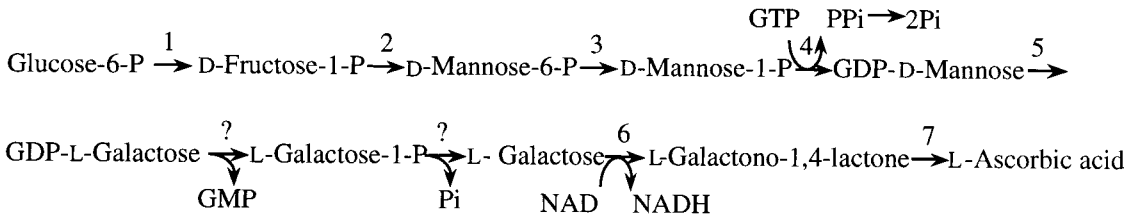

FIG. 1. Proposed pathway for AsA biosynthesis in higher plants (2). Enzymes: 1, phosphoglucose isomerase; 2, phosphomannose isomerase; 3, phosphomannomutase; 4, GDP-D-mannose pyrophosphorylase; 5, GDP-D-mannose-3,5-epimerase; 6, L-galactose dehydrogenase; 7, L-galactono-1,4-lactone dehydrogenase.

≈25% relative humidity) under a 16-hr photoperiod. Before transformation by vacuum infiltration, plants were grown under a 12-hr photoperiod with other conditions as described (15). T_2 transgenics were germinated on sterile plant nutrient medium as described (16) and then transplanted to soil and grown under the same conditions as the T_1 transgenics. The tissues used for the tracer study and GDP-mannose pyrophosphorylase activity assay were from plants grown in a greenhouse in Exeter, U.K., as described (13). All experiments using *vtc1-1* were performed on a line that had been backcrossed to the wild-type (wt) Col-0 progenitor four times.

D-[U-^{14}C] Mannose Tracer Study. The labeling of *vtc1-1* and wt Col-0 leaves with D-[U-^{14}C] mannose via the transpirational stream, fractionation of the labeled extracts, and further purification of L-[^{14}C-AsA] by HPLC were done as described (2, 13).

***VTC1* Locus Mapping.** The *VTC1* locus was mapped onto the *Arabidopsis* genome with 414 *vtc1-1*/*vtc1-1* individuals developed from an F_2 mapping population derived from a cross with the *Ler* ecotype. Molecular markers used in this mapping included the cleaved amplified polymorphic sequence markers m429 (17) and 178 (18) and the microsatellite marker nga168 (19).

GDP-Mannose Pyrophosphorylase Assay. GDP-mannose pyrophosphorylase activity was assayed in the reverse direction in crude extracts that were prepared by extraction of 0.3 g of leaf tissue in 1 ml of 100 mM Tris (pH 7.6), 1% polyvinylpyrrolidone, 5 mM DTT, and 1 mM EDTA followed by centrifugation to remove insoluble material. The reactions were performed by adding 30 μl of crude extract to 104 μl of 15.4 mM $MgCl_2$, 15.4 mM NaPPi, 13.5 mM Tris·HCl (pH 8.0), 1.1 mM EDTA, and 0.1 μCi GDP-[^{14}C]-mannose (1 Ci = 37 GBq; Amersham) and were terminated by boiling. The reactions were clarified by centrifugation and then lyophilized. For separation of the nucleotide sugars from the sugar phosphates by TLC, the samples were resuspended in dH_2O, and a fifth of each sample was spotted onto cellulose plates (150 μm, K2 cellulose; Whatman). The separation solvent was ethanol/1 M ammonium acetate, pH 5.0 (60:40 by volume). To detect radioactivity, the TLC plates were scanned with a Berthold Linear Analyzer (model LB2832, Berthold, Hempstead, U.K.). The identification of nucleotide sugars and sugar phosphates were determined first by comparison to a comigrating GDP-[^{14}C]-mannose standard and second by staining plates with an ammonium molybdate stain (20). The nucleotide sugars and sugar phosphates were scraped off the cellulose plates and eluted from the cellulose in dH_20. The free sugars were released by hydrolysis and analyzed as described (2). Protein concentrations were determined by the Bradford assay with γ-globulin as a control.

The *Arabidopsis* leaf extracts contained a potentially interfering phosphodiesterase activity that produced mannose-1-P and GMP from GDP-mannose. However this phosphodiesterase activity was completely inhibited by the high PP_i concentration used in the pyrophosphorylase assay. This inhibition of phosphodiesterase by PP_i was confirmed by experiments with bovine intestinal mucosa phosphodiesterase 1 (Sigma) under the same conditions as the pyrophosphorylase assay.

cDNA and Mutant Allele Sequence Analyses. The cDNA encoding the *Arabidopsis* GDP-mannose pyrophosphorylase [expressed sequence tag (EST) ID no. 9908, GenBank accession no. T46645] was obtained from the *Arabidopsis* Biological Resource DNA Stock Center (aims.cps.msu.edu/aims; Columbus, OH). This cDNA was fully sequenced on both strands.

The mutant alleles *vtc1-1* and *vtc1-2* were sequenced from PCR amplification products of genomic DNAs. For each mutant allele, an ≈1.4-kb *Bgl*II fragment containing the majority of the coding region was sequenced by using the primers, 5′-TGGTAAATACGCACTCAAT-3′ (named 5′-GMP) and 5′-AAAACAGCAAACGACCCTAACAA-3′ (named 3′-GMP). To confirm the public domain sequence of bacterial artificial chromosome (BAC) T5I7 that included the base mutated in the *vtc1* alleles, both strands of a portion of a Col-0 wt *VTC1 Cla*I genomic clone (described below) were sequenced. The sequence of *VTC1*, *vtc1-1*, and *vtc1-2* that included exon 1 and intron 1 was obtained directly from genomic DNA amplified with 5′-GMP and 5′-CATTCTTGT-TGGAGGCTTCGG-3′. The sequence downstream of the *Bgl*I fragment for *vtc1-1* and *vtc1-2* was obtained from genomic DNA amplified with the 5′-GAATAAGCATCAAT-CAAAACGC-3′ and 5′-GCTAAGACCGACTTCAATCG-3′. More than one independent PCR product was sequenced to confirm the veracity of the data.

Complementation Analysis. A 5.4-kb *Cla*I fragment containing the *VTC1* locus was subcloned from BAC T5I7. A 3.4-kb fragment from this subclone was then ligated into the binary vector pGPTV-BAR/*Hin*dIII (21). This construct (g*VTC1*-pGPTV) was transformed into *Agrobacterium tumefaciens* pMP90 strain GV3101 and introduced into *vtc1-1* plants by vacuum infiltration. Glufosinate-ammonium resistant T_1 transgenic individuals were selected by sowing seeds and spraying the soil surface with 500 ml/m^2 of 0.25 mg ml^{-1} commercially formulated glufosinate-ammonium (Finale; AgrEvo, Montvale, NJ). Twelve days after sowing, resistant T_1 seedlings were transplanted to nontreated soil and allowed to self-pollinate. T_2 progeny were scored for glufosinate-ammonium resistance by painting individual leaves with the herbicide (150 μg ml^{-1} glufosinate-ammonium, 250 nl ml^{-1} Silwet). These plants were also scored for wt or mutant (deficient) levels of AsA by a nitroblue tetrazolium-based method in which single leaves are squashed onto chromatography paper and treated with 1 mg/ml of nitroblue tetrazolium. The AsA in wt leaves is sufficient to reduce the nitroblue tetrazolium to the visible precipitate formazan, whereas no readily visible formazan is produced upon treatment of *vtc1-1* leaves (P.L.C. *et al.*, unpublished data). AsA levels were then confirmed by a previously described spectrophotometric-based assay (12).

RESULTS

The *Arabidopsis vtc1-1* mutant was isolated from ethyl methanesulfonate (EMS) mutagenized Col-0 wt plants by virtue

of its ozone sensitivity. *vtc1-1* contains ≈25% of wt AsA concentrations, and previously reported results strongly suggest that this deficiency is because of a defect in AsA biosynthesis (12, 13). This mutant was used as a tool to identify the *VTC1* gene.

Conversion of AsA from D-Mannose Is Reduced in *vtc1-1*. It is well established that D-glucose is a precursor to AsA and our previous results showed that *vtc1-1* is defective in the conversion of D-glucose to AsA (12). As D-mannose is a biosynthetic intermediate in the newly proposed pathway (Fig. 1; ref. 2) feeding studies were conducted to ask whether *vtc1-1* has a decreased ability to convert D-[U-^{14}C]mannose to ^{14}C-AsA. Excised leaves were fed with D-[U-^{14}C]mannose through the transpirational stream for 1.5 hr and then transferred to water for 4 hr. AsA was fractionated from extracts of these labeled leaves, and the amount of ^{14}C-AsA was then determined and expressed as a percent of ^{14}C in the total soluble fraction. As shown in the HPLC traces in Fig. 2, a greater percentage of ^{14}C was present as L-[^{14}C]AsA in wt than *vtc1-1* in every sample. Approximately 6.6% of the total ^{14}C was present as L-[^{14}C]AsA in the wt samples compared with ≈2.6% in the *vtc1-1* samples. Therefore, the AsA-deficient mutant *vtc1-1* is defective in the conversion of D-mannose to AsA. These data strongly support the proposal that D-mannose is a substrate for AsA biosynthesis and that *vtc1-1* is defective in one of the activities responsible for conversion of mannose to AsA.

Identification of a Putative *VTC1* Gene on BAC T5I7. By using a mapping population of >400 F_3 families derived from a cross between *vtc1-1* and the wt L*er* ecotype, *VTC1* was fine-mapped to a position on chromosome 2 to one side of two molecular markers; 0.9 centimorgan (cM) from marker m429 (17) and 1.2 cM from marker nga168 (19) as shown in Fig. 3*A*. By using microsatellite marker 178, which is >1 cM centromeric proximal to nga168 (18), we determined that *VTC1* is centromere distal to nga168 and m429. All seven *vtc1/vtc1* mapping lines that were recombinant between nga168 and *VTC1* were also recombinant for marker 178 (including two between m429 and nga168), indicating that the relative order of these loci is as shown. This map is inconsistent with public domain recombinant inbred results, presumably because of the limited resolution of the recombinant inbred map: m429 is reported as being centromere proximal to nga168 (http://nasc.nott.ac.uk/new_ri_map.html). Our mapping data place *VTC1* within a 2 Mb region on Chr 2 that spans m429 to just beyond marker m336, which is currently being sequenced by the Institute for Genomic Research (TIGR). The sequence of a 92-kb BAC (T5I7) within that contig (Fig. 3*B*) was annotated by TIGR and the ORF T5I7.7 was identified as a putative mannose-1-phosphate guanyltransferase (www.tigr.org/docs/tigr-scripts/bac_scripts/bac_display.spl?bac_name=T5I7). An alias for this enzyme is GDP-mannose pyrophosphorylase, which catalyzes step 4 in the proposed AsA biosynthetic pathway shown in Fig. 1. In this reaction, mannose-1-P is converted to GDP-mannose, with the consumption of GTP and the release of PPi.

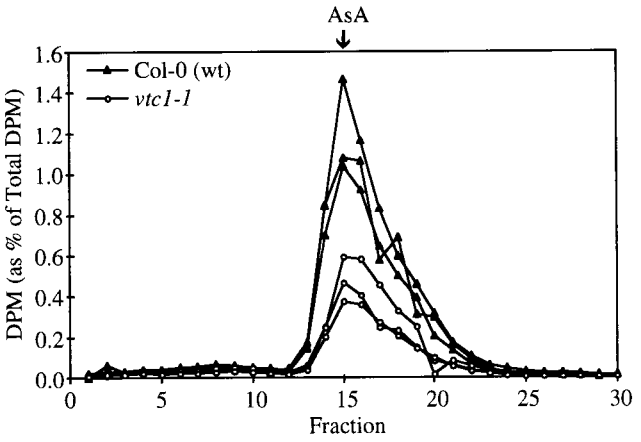

FIG. 2. The incorporation of ^{14}C from D-[U-^{14}C]mannose into ^{14}C-AsA by *Arabidopsis* leaves is less in *vtc1-1* (○) than wt (▲). Excised leaves were labeled with D-[U-^{14}C]mannose. The AsA-containing fraction from soluble extracts of these leaves was fractionated by HPLC. The AsA peak was collected in 30 fractions, which were individually assayed for ^{14}C. The results are expressed as a percentage of total ^{14}C incorporated into AsA. Three replicate samples were processed for each genotype.

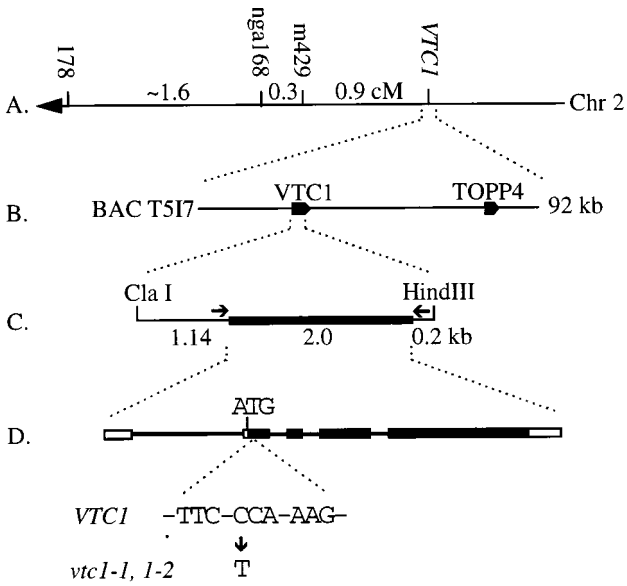

FIG. 3. Genetic and physical characterization of the *VTC1* locus. (*A*) *VTC1* was mapped to a position on chromosome 2, 0.9 cM centromere distal from cleaved amplified polymorphic sequence (CAPS) marker m429, placing it within a sequenced region of the genome. (*B*) A gene encoding a putative GDP-mannose pyrophosphorylase is located on the 92-kb BAC T5I7 at the centromere proximal end of this contig. The relative map positions of the *VTC1* locus and a second genetically identified locus, *TOPP4*, on BAC T5I7 are shown. (*C*) The ≈3.4-kb *Cla*I–*Hin*dIII fragment from this BAC used to complement the *vtc1-1* mutation by *Agrobacterium*-mediated transformation. The location of oligonucleotide primers used to amplify the *VTC1* locus from *vtc1-1* and *vtc1-2* genomic DNA for sequence analysis are indicated with arrows. (*D*) The structure of the *VTC1* transcribed region is shown along with the nucleotide substitution in *vtc1-1* and *vtc1-2*; unshaded rectangles, noncoding sequences present in the *VTC1* cDNA; shaded rectangles, exons encoding the GDP-mannose pyrophosphorylase; thin lines, the location of intron sequences.

Partial sequence for a GDP-mannose pyrophosphorylase cDNA, also annotated as encoding a putative mannose-1-phosphate guanyltransferase, had been previously reported (EST ID #9908; www.ncbi.nlm.nih.gov/irx/cgi-bin/birx_doc?dbest_cu+6850). We determined the sequence of a full-length cDNA encoding this protein to define all intron/exon borders and found that this gene contains 5 exons with exon 1 and a small section of exon 2 being a 5′ untranslated region. The ≈40-kDa protein inferred from this ORF has 59% amino acid identity with the mannose-1-phosphate guanyltransferase from *Saccharomyces cerevisiae*. As described below, we have collected biochemical, molecular, and genetic evidence in support of the hypothesis that the *VTC1* vitamin C biosynthetic locus encodes a GDP-mannose pyrophosphorylase.

***vtc1-1* Is Deficient in GDP-Mannose Pyrophosphorylase Activity.** If *VTC1* encodes GDP-mannose pyrophosphorylase, the AsA-deficient mutant *vtc1-1* would be predicted to have reduced enzyme activity compared with wt plants. As the activity of this enzyme is fully reversible *in vitro*, pyrophosphorylase activity can be assayed by monitoring the production

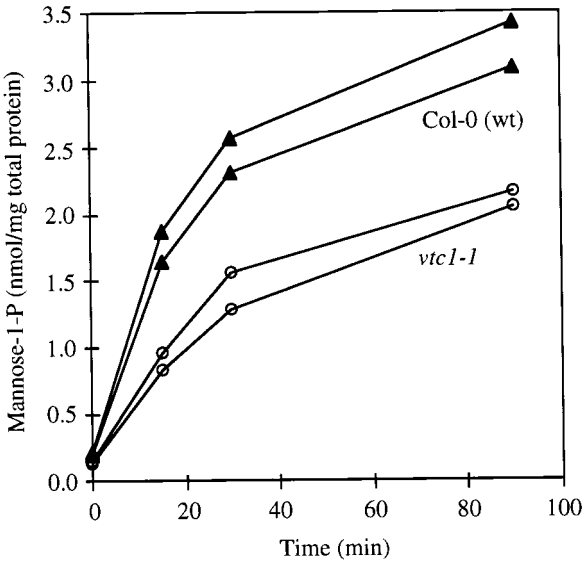

FIG. 4. The activity of GDP-mannose pyrophosphorylase is lower in *vtc1-1* than wt. Enzyme activity was measured in the reverse direction by PP_i-dependent formation of ^{14}C-mannose-1-P from GDP-[U-^{14}C]mannose. The values are from assays of two independent leaf extracts per genotype. ▲, wt extracts; ○, *vtc1-1* extracts.

of mannose-1-P from GDP-mannose and PPi (22). This assay was used to measure GDP-mannose pyrophosphorylase activity in extracts from both *vtc1-1* and wt. As shown in Fig. 4, the time-dependent production of mannose-1-P from GDP-mannose and PPi is lower in extracts from *vtc1-1* than wt. After a 90-min incubation, ≈35% less mannose-1-P is formed in *vtc1-1* compared with wt.

***vtc1-1* and *vtc1-2* Contain a Mutation in the Gene Encoding GDP-Mannose Pyrophosphorylase.** To test the hypothesis that *vtc1-1* and *vtc1-2* (the isolation of *vtc1-2* is described by P.L.C. *et al.*, unpublished data) harbor mutations in the GDP-mannose pyrophosphorylase gene, we looked for mutations in the pyrophosphorylase genomic sequence derived from each of these mutant alleles. Indeed, the sequences of both *vtc1-1* and *vtc1-2* contain the identical single cytosine to thymine point mutation at position +64 relative to the first base of the

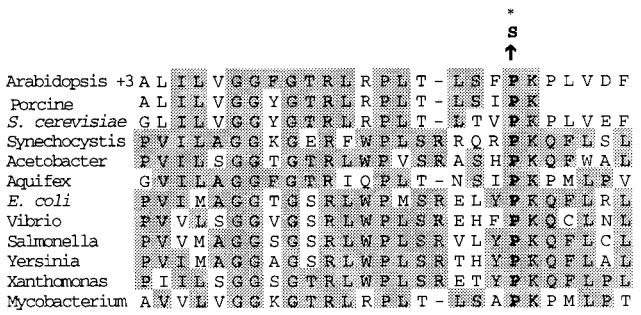

FIG. 5. Comparison of the N-terminal portion of the *Arabidopsis* GDP-mannose pyrophosphorylase with the analogous portion of the enzyme from other organisms. The following are the GenBank accession numbers for the GDP-mannose pyrophosphorylase sequences aligned with the *Arabidopsis* pyrophosphorylase: *Saccharomyces cerevisiae,* 1431053; *Synechocystis sp.*, 1653346; *Acetobacter xylinus,* 2569943; *Aquifex aeolicus,* 2983302; *Escherichia coli,* 3142209; *Vibrio cholerae,* 1230580; *Salmonella typhimurium,* 117277; *Yersinia enterocolitica,* 1197654; *Xanthomonas campestris,* 267418; and *Mycobacterium tuberculosis,* 1877319. Note that the porcine (*Sus scrofa domestica*, 476970) sequence is from N-terminal sequence data obtained from the B chain of GDP-mannose pyrophosphorylase. The proline highlighted in boldface (**P**) is the wt amino acid converted to a serine (→**S**) in *vtc1-1* and *vtc1-2*.

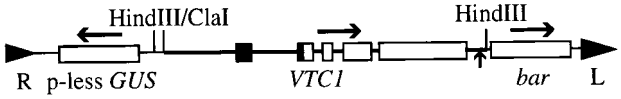

FIG. 6. The structure of the T-DNA construct used to complement the *vtc1-1* mutation. An ≈3.4-kb *Cla*I–*Hin*dIII fragment that contains the *VTC1* gene including ≈1.1 kb upstream of the start of the *VTC1* cDNA (including the nontranslated exon 1 and nontranslated section of exon 2, ■), the four protein-encoding exons (□) and the poly(A)$^+$ site identified in the cDNA (↑), to a site 0.23 kb downstream of the stop codon was cloned into the binary vector pGPTV-BAR (21) and used to generate transgenic *vtc1-1* plants. This vector also contains a copy of the *bar* gene (□) and a promoterless GUS (□) between the left and right T-DNA borders (L, R). →, The orientations of *VTC1*, *bar*, and the promoterless GUS.

presumed initiator methionine (Fig. 3*D*). This predicted missense mutation would convert a highly conserved proline to a serine at amino acid 22 in the GDP-mannose pyrophosphorylase amino acid sequence (Fig. 5).

The point mutation in the *vtc1* mutants does not alter the GDP-mannose pyrophosphorylase mRNA level. RNA filter hybridization analysis revealed no significant difference in the steady-state level of the GMP-encoding mRNA (data not shown) in *vtc1-1*, *vtc1-2* and wt. These results are consistent with the hypothesis that the proline to serine change at amino acid position 22 affects the enzyme activity or stability rather than transcription or mRNA stability.

DNA Encoding the wt GDP-mannose Pyrophosphorylase Complements the *vtc1-1* Mutation in Transgenic Plants. To verify that the *VTC1* locus encodes GDP-mannose pyrophosphorylase, we asked whether a wt copy of this locus introduced as a transgene would complement the *vtc1-1* allele and restore normal levels of AsA. A genomic clone including ≈1.1 kb upstream of the 5′ end of the GDP-mannose pyrophosphorylase cDNA and ≈0.2 kb downstream of the predicted stop codon (Figs. 3*C* and 6) was subcloned from BAC T5I7 and transformed into *vtc1-1* plants by the *Agrobacterium tumefaciens* vacuum infiltration method. T_1 transgenic plants were selected by glufosinate-ammonium resistance conferred by the BAR gene. Thirteen glufosinate-ammonium resistant T_1 transgenics that were confirmed to contain the BAR gene by PCR amplification all contained wt levels of AsA. These results were consistent with the hypothesis that the transgene complemented *vtc1-1*. The T_1 lines were allowed to self-pollinate and three selected T_2 lines from independent T_1 lines were tested for cosegregation of wt levels of AsA (scored by using a qualitative AsA assay) and glufosinate-ammonium resistance. Introduction of the *VTC1* locus into the AsA-deficient *vtc1-1* mutant confers increased levels of AsA that cosegregate with

Table 1. Cosegregation of elevated AsA levels and the selectable marker in *vtc1-1* lines transformed with genomic copy(s) of the *VTC1* locus

Line	AsA+ *no. Basta^r/total†	AsA− no. Basta^r/total
1	79 (10/10)	28 (1/11)
2	70 (10/10)	34 (0/12)
3	75 (11/11)	29 (0/10)

AsA levels were scored by using a nitroblue tetrazolium-based visual method in three independent lines of segregating T_2 generation plants obtained from self-pollination of glufosinate-ammonium resistant T_1 individuals. Two-week-old plants were scored as AsA positive (+) if a single leaf treated with nitroblue tetrazolium (1 mg/ml) produced a visually similar amount of formazan (from reduction by AsA) as wt, whereas plants were scored as AsA negative (−) if the formazan precipitate was virtually absent. For each T_2 line, 10–12 individuals from both AsA (+) and AsA (−) classes were then tested for resistance to the selectable marker. Basta^r, glufosinate-ammonium resistant.

the selectable marker (Table 1). Finally, 10 individuals that scored as wt for AsA from each T_2 line were pooled, extracts were prepared, and total AsA was measured by using a quantitative spectrophotometric assay. These pooled extracts contained between 2.4 and 3.8 μmol of AsA per g of fresh weight (FWT), of AsA which is similar to the 3.1 μmol of AsA per g of FWT seen in wt, and greater than the 0.9 μmol of AsA per g of FWT in the mutant. Together, these results confirm that the *VTC1* locus encodes a GDP-mannose pyrophosphorylase structural gene.

DISCUSSION

GDP-mannose pyrophosphorylase is an enzyme in the recently proposed plant AsA biosynthetic pathway (Fig. 1; ref. 2). We have presented conclusive evidence that this enzyme is encoded by the *VTC1* locus in *Arabidopsis*. First, the AsA-deficient *vtc1-1* mutant is defective in the conversion of mannose to AsA. Second, the activity of GDP-mannose pyrophosphorylase is lower in extracts from *vtc1-1* than wt. Third, the *VTC1* locus genetically maps to a region of genomic DNA encoding a GDP-mannose pyrophosphorylase homologue and the *vtc1-1* and *vtc1-2* mutants each harbor the identical point mutation that alters a highly conserved proline residue in this gene. Finally, a transgene encoding the wt pyrophosphorylase genetically complements the *vtc1-1* mutation, increasing the AsA in the transgenic *vtc1-1* lines to levels similar to wt. These results strongly support the assertion that the AsA biosynthetic pathway proposed based on *in vitro* biochemical data also operates *in vivo*.

In addition to *VTC1* in *Arabidopsis*, genes encoding GDP-mannose pyrophosphorylase have been described from a variety of organisms including eubacteria such as *Escherichia coli* (23), *Acetobacter xylinum* (24), and *Pseudomonas aeruginosa* (25) and the yeast *S. cerevisiae* (26). ESTs predicted to encode GDP-mannose pyrophosphorylase have been identified in rice and cotton (GenBank accession nos. C91653 and AI055222). Unlike plants and yeast, some eubacteria such as *P. aeruginosa* and *A. xylinum* encode bifunctional enzymes with both phosphomannose isomerase and GDP-mannose pyrophosphorylase activities (Fig. 1, steps 2 and 4; refs. 24 and 27), whereas others such as *E. coli* encode these activities on separate genes (28, 29). In the eubacteria, genes involved in GDP-mannose biosynthesis can be located together on an operon. For example, the gene encoding GDP-mannose pyrophosphorylase in *Salmonella enterica* is part of the *rfb* operon that also encodes phosphomannomutase (Fig. 1, step 3; ref. 30).

Apart from vitamin C biosynthesis in plants, the activated form of mannose, GDP-mannose, is used in a number of diverse cellular processes. Both prokaryotes and eukaryotes utilize GDP-mannose in the synthesis of complex structural carbohydrates. Mannose (obtained from GDP-mannose) is a component of microbial lipopolysaccharides, which are the major component of the outer wall of most Gram-negative bacteria, and exopolysaccharides, long chain polymers that are secreted by a number of different classes of bacteria. Similarly, GDP-mannose also contributes to the synthesis of three different structural carbohydrates in plant cell walls. First, hemicellulose polymers such as glucomannans and galactomannans, contain D-mannose that is derived from its activated form. Mannans are major wall-based carbohydrate stores in some seeds (31). Second, GDP-mannose is the substrate for GDP-D-mannose-4,6-dehydratase, an enzyme that catalyzes the first step in GDP-L-fucose biosynthesis, which is encoded by the *MUR1* gene of *A. thaliana* (32). L-Fucose is present in both plant cell walls and on glycoproteins. Finally, L-galactose, a minor component of plant cell walls, is synthesized from GDP-mannose (2, 7). In addition to a major function in structural carbohydrate biosynthesis, GDP-mannose also has a key role in protein glycosylation in eukaryotes. D-mannose, the major carbohydrate component of both *N*- and *O*-linked glycoproteins, is derived from GDP-mannose during the glycosylation process.

Because of the many functions of GDP-mannose in plant cells, a deficiency in the synthesis of this activated sugar would be expected to result in a number of different biochemical defects. We have shown that the AsA-deficient *vtc1* mutant is deficient in GDP-mannose pyrophosphorylase activity, suggesting the possibility that *vtc1* is also deficient in other products derived from GDP-mannose. Indeed, preliminary evidence suggests that *vtc1-1* has an altered glycosylated protein profile (P.L.C. and R.L.L., data not shown). If the *vtc1-1* mutant is deficient in GDP-mannose, an alteration in cell wall carbohydrates might also result.

Because GDP-mannose plays roles in many different essential cellular processes, it is expected that a null mutation abolishing GDP-mannose pyrophosphorylase activity would be lethal. The *Arabidopsis* mutant *cyt1-2* was recently found to contain a mutation in the GDP-mannose pyrophosphorylase gene, which is predicted to abolish its function (W. Lukowitz and C. R. Somerville, personal communication). *cyt1-2* is an embryo-lethal mutant, arresting at a very early stage in embryonic development with severely abnormal cell walls (33), providing strong evidence for the lethality of a severe GDP-mannose pyrophosphorylase deficiency. Mutants with known or predicted GDP-mannose deficiencies have also been described in yeast and humans. A null mutant generated by gene disruption of the *S. cerevisiae* GDP-mannose pyrophosphorylase (*VIG9*) gene was lethal in the haploid state, indicating that *VIG9* is essential for growth in yeast (26). Patients with carbohydrate-deficient glycoprotein syndrome type 1A (Jaeken syndrome) have deficiencies in phosphomannomutase (Fig. 1, step 3) and are predicted to have GDP-mannose deficiency. Overall, 20% of patients diagnosed with this syndrome die within the first few years of life (34). The most frequent mutant allele appears to be lethal as it has not been found in the homozygous state and other patients carrying two different mutant alleles have a high mortality rate (35).

Although a null mutation that abolishes GDP-mannose pyrophosphorylase activity is lethal in yeast and *Arabidopsis*, it is possible to isolate nonlethal mutants with proven or predicted GDP-mannose deficiencies. In addition to the *Arabidopsis vtc1* mutant, such mutants have been described in both yeast and humans. The *S. cerevisiae* GDP-mannose pyrophosphorylase mutant *vig9-1* is viable yet protein glycosylation-deficient. This mutant still contains 70% of wt intracellular GDP-mannose (26). Some patients with Jaeken syndrome are homozygous for one of two different mutations in the phosphomannomutase gene, suggesting that the effects of these mutations are relatively mild (35).

It is interesting to note that the *Arabidopsis vtc1-1* and *vtc1-2* mutants contain the exact same point mutation in *VTC1* despite having been independently isolated from different EMS-mutagenized pools. This suggests that there are a limited number of different mutations tolerated by this enzyme in plants without causing the embryo-lethal phenotype. Indeed, several different *cyt1* alleles (including *cyt1-1*)have been identified among collections of embryonic lethals. The independently isolated *cty1-1* and *cyt1-2* mutants are known to contain mutations at different amino acids in the GDP-mannose pyrophosphorylase gene (W. Lukowitz, S. Gillmor, A. Roeder, and C. Somerville, personal communication). Another example of such an allelic constraint is documented in the *Arabidopsis* literature. Four *Arabidopsis* feedback-resistant mutants of anthranilate synthase that were independently isolated in two different laboratories were all found to contain the same amino acid substitution, suggesting severe constraints on changing allosteric regulation while maintaining catalytic activity (36, 37).

We predict that a severe mutation specifically abolishing AsA synthesis in plants would be lethal because of the diverse and critical functions of AsA. Indeed, AsA-deficient *Arabidopsis* mutants describing three new *VTC* loci have been recently isolated yet none of these mutants eliminate AsA entirely (P.L.C. *et al*., unpublished data). Although no higher plant mutants have yet been described that are known to affect only AsA biosynthesis, analogous mutants do exist in the animal kingdom. The enzyme L-gulono-1,4-lactone dehydrogenase catalyzes the synthesis of AsA from L-gulono-1,4-lactone in animals. Several vertebrates completely lack this activity including guinea pigs, pigeons, bats, and primates (including humans) and therefore are unable to synthesize AsA. AsA must be provided in the diet of these animals or this deficiency is lethal (38).

This study highlights the utility of combining methodologies from the fields of classical genetics and modern genomics. Traditional genetic techniques such as screening mutants generated by EMS mutagenesis for specific phenotypes have proven to be valuable methods for isolation of genes involved in basic metabolic processes. The ''leaky'' alleles created by a single base mutation in *VTC1* allowed us to recover living plants selected by virtue of their ozone sensitivity (*vtc1-1*; ref. 12) or AsA-deficiency (*vtc1-2*; P.L.C. *et al*., unpublished data) despite the apparent need for this enzyme activity in embryonic development. The traditional map-based cloning of genes is being greatly facilitated by the large volumes of sequence and high resolution genetic maps available for the *Arabidopsis* genome. The powerful candidate gene approach of rapidly associating a mutant phenotype with a gene, in this case predicted from the proposed AsA biosynthetic pathway, was facilitated by this wealth of sequence information. EST data permitted us to rapidly obtain cDNAs encoding a putative GDP-mannose pyrophosphorylase, and the sequence data on Chr II generated as part of the *Arabidopsis* Genomics Initiative enabled the rapid identification of the candidate gene for *VTC1*. Such available sequence data will also no doubt facilitate the fine-mapping and identification of the other *VTC* loci, allowing us to obtain an even clearer picture of AsA biosynthesis in higher plants.

This work was supported by Grant 96-35100-3212 from the Plant Responses to the Environment Program of the National Research Initiative Competitive Grants Program, U.S. Department of Agriculture (to R.L.L. and P.L.C.); and by a Biotechnology and Biological Science Research Council Postgraduate Studentship (to G.L.W.).

1. Smirnoff, N. (1996) *Ann. Bot.* **78,** 661–669.
2. Wheeler, G. L., Jones, M. A. & Smirnoff, N. (1998) *Nature (London)* **393,** 365–369.
3. Loewus, F. A. (1988) in *The Biochemistry of Plants: Carbohydrates*, ed. Priess, J. (Academic, New York), Vol. 14, pp. 85–107.
4. Loewus, F. A. (1963) *Phytochemistry* **2,** 109–128.
5. Loewus, M. W., Bedgar, D. L., Saito, K. & Loewus, F. A. (1990) *Plant Physiol.* **94,** 1492–1495.
6. Saito, K., Nick, J. A. & Loewus, F. A. (1990) *Plant Physiol.* **94,** 1496–1500.
7. Barber, G. A. (1971) *Arch. Biochem. Biophys.* **147,** 619–623.
8. Barber, G. A. (1979) *J. Biol. Chem.* **254,** 7600–7603.
9. Ôba, K., Ishikawa, S., Nishikawa, M., Mizuno, H. & Yamamoto, T. (1995) *J. Biochem. (Tokyo)* **117,** 120–124.
10. Østergaard, J., Persiau, G., Davey, M. W., Bauw, G. & Van Montagu, M. (1997) *J. Biol. Chem.* **272,** 30009–30016.
11. Mutsuda, M., Ishikawa, T., Takeda, T. & Shigeoka, S. (1995) *Biosci. Biotechnol. Biochem.* **59,** 1983–1984.
12. Conklin, P. L., Williams, E. H. & Last, R. L. (1996) *Proc. Natl. Acad. Sci. USA* **93,** 9970–9974.
13. Conklin, P. L., Pallanca, J. E., Last, R. L. & Smirnoff, N. (1997) *Plant Physiol.* **115,** 1277–1285.
14. Landry, L. G., Chapple, C. C. S. & Last, R. L. (1995) *Plant Physiol.* **109,** 1159–1166.
15. Conklin, P. L. & Last, R. L. (1995) *Plant Physiol.* **109,** 203–212.
16. Li, J., Zhao, J., Rose, A. B., Schmidt, R. & Last, R. L. (1995) *Plant Cell* **7,** 447–461.
17. Konieczny, A. & Ausubel, F. M. (1993) *Plant J.* **4,** 403–410.
18. Li, J., P., N., Vitart, V., McMorris, T. & Chory, J. (1996) *Science* **272,** 398–401.
19. Bell, C. J. & Ecker, J. R. (1994) *Genomics* **19,** 137–144.
20. Dawson, R. M. C., Elliot, D. C., Elliot, W. H. & Jones, K. M. (1986) in *Data for Biochemical Research* (Oxford Univ. Press, London), 3rd Ed., pp. 485–486.
21. Becker, D., Kemper, E., Schell, J. & Masterson, R. (1992) *Plant Mol. Biol.* **20,** 1195–1197.
22. Szumilo, T., Drake, R. R., York, J. L. & Elbein, A. D. (1993) *J. Biol. Chem.* **268,** 17943–17950.
23. Sugiyama, T., Kido, N., Komatsu, T., Ohta, M., Jann, K., Jann, B., Saeki, A. & Kato, N. (1994) *Microbiology* **140,** 59–71.
24. Griffin, A. M., Poelwijk, E. S., Morris, V. J. & Gasson, M. J. (1997) *FEMS Microbiol. Lett.* **154,** 389–396.
25. Sa-Correia, I., Darzins, A., Wang, S.-K., Berry, A. & Chakrabarty, A. M. (1987) *J. Bacteriol.* **169,** 3224–3231.
26. Hashimoto, H., Sakakibara, A., Yamasaki, M. & Yoda, K. (1997) *J. Biol. Chem.* **272,** 16308–16314.
27. Shinabarger, D., Berry, A., May, T. B., Rothmel, R., Fialho, A. & Chakrabarty, A. M. (1991*) J. Biol. Chem*. **266,** 2080–2088.
28. Jayaratne, P., Bronner, D., Maclachlan, P. R., Dodgson, C., Kido, N. & Whitfield, C. (1994) *J. Bacteriol.* **176,** 3126–3139.
29. Miles, J. S. & Guest, J. R. (1984) *Gene* **32,** 41–48.
30. Jiang, X.-M., Neal, B., Santiago, F., Lee, S. J., Romano, L. K. & Reeves, P. R. (1991) *Mol. Microbiol*. **5,** 695–713.
31. Bewley, J. D., Burton, R. A., Morohashi, Y. & Fincher, G. B. (1997) *Planta* **203,** 454–459.
32. Bonin, C. P., Potter, I., Vanzin, G. F. & Reiter, W.-D. (1997) *Proc. Natl. Acad. Sci. USA* **94,** 2085–2090.
33. Nickle, T. C. & Meinke, D. W. (1998) *Plant J.* **15,** 321–332.
34. Matthijs, G., Schollen, E., Pardon, E., Veiga Da Cunha, M., Jaeken, J., Cassiman, J. J. & Van Schaftingen, E. (1997) *Nat. Genet.* **16,** 88–92.
35. Matthijs, G., Schollen, E., Van-Schaftingen, E., Cassiman, J.-J. & Jaeken, J. (1998) *Am. J. Hum. Genet.* **62,** 542–550.
36. Li, J. & Last, R. L. (1996) *Plant Physiol.* **110,** 51–59.
37. Kreps, J. A., Ponappa, T., Dong, W. & Town, C. D. (1996) *Plant Physiol.* **110,** 1159–1165.
38. Padh, H. (1990) *Biochem. Cell. Biol.* **68,** 1166–1173.